Konya Mühendislik Bilimleri Dergisi, c. 11, s. 1, 10-20, 2023
Konya Journal of Engineering Sciences, v. 11, n. 1, 10-20, 2023
ISSN: 2667-8055 (Electronic)
DOI: 10.36306/konjes.1172687

OPTIMAL PID CONTROLLER DESIGN FOR TRAJECTORY TRACKING OF A DODECAROTOR UAV BASED ON GREY WOLF OPTIMIZER

[1]Şahin YILDIRIM, [2*]Nihat ÇABUK, [2,3]Veli BAKIRCIOĞLU

[1] *Erciyes University, Engineering Faculty, Mechatronics Engineering Department, Kayseri, TÜRKİYE*
[2] *Aksaray University, Vocational School of Technical Sciences, Aksaray, TÜRKİYE*
[3] *Middle East Technical University, Center for Robotics and AI (ROMER), Ankara, TÜRKİYE*
[1]sahiny@erciyes.edu.tr, [2]nihatcabuk@aksaray.edu.tr, [3]vbakirci@metu.edu.tr

Highlights

- A cascaded PID control algorithm was employed to control the proposed dodecarotor,
- Obtained optimal gains of the controllers for the position and orientation of the proposed dodecarotor,
- Auto-tuning of gains was done comparatively based on PSO and GWO algorithms.

***Corresponding Author:** Nihat ÇABUK, nihatcabuk@aksaray.edu.tr

Konya Mühendislik Bilimleri Dergisi, c. 11, s. 1, 10-20, 2023
Konya Journal of Engineering Sciences, v. 11, n. 1, 10-20, 2023
ISSN: 2667-8055 (Electronic)
DOI: 10.36306/konjes.1172687

OPTIMAL PID CONTROLLER DESIGN FOR TRAJECTORY TRACKING OF A DODECAROTOR UAV BASED ON GREY WOLF OPTIMIZER

[1]Şahin YILDIRIM, [2*]Nihat ÇABUK, [2,3]Veli BAKIRCIOĞLU

[1] *Erciyes University, Engineering Faculty, Mechatronics Engineering Department, Kayseri, TÜRKİYE*
[2,3] *Aksaray University, Vocational School of Technical Sciences, Aksaray, TÜRKİYE*
[3] *Middle East Technical University, Center for Robotics and AI (ROMER), Ankara, TÜRKİYE*
[1]sahiny@erciyes.edu.tr, [2]nihatcabuk@aksaray.edu.tr, [3]vbakirci@metu.edu.tr

(Received: 10.09.2022; Accepted in Revised Form: 01.11.2022)

ABSTRACT: In this study, we aimed to find optimal PD controller gains to control orientation and position of a Dodecarotor UAV with minimum trajectory error. In this context, a cascaded PD controller approach which has velocity feedback in the inner loop and position feedback in the outer loop was adopted for each state (roll, pitch, yaw, altitude) in the flight control of the UAV. Subsequently, a fitness function was defined based on the system's time domain response and trajectory tracking error for each state, except the yaw angle, which is non-dominant in terms of trajectory tracking performance. Grey Wolf Optimizer (GWO) was used to obtain PD gains by minimizing the defined fitness function. At the same time, Particle Swarm Optimizer was used in order to benchmark the obtained results from GWO and to avoid a shallow solution space. The obtained PD controller parameters as a result of the optimization study of both algorithms were implemented to the system and the results were compared with each other. Finally, the gains that provided the best results for both algorithms were compared with each other and the results were discussed in terms of the time domain results and the actuator input smoothness. It has been observed that the GWO optimized controller provides a 40-46% improvement over PSO in all four different mass UAVs in terms of reducing axis position errors.

Keywords: *PID control, GWO, Optimization, UAV*

1. INTRODUCTION

Unmanned aerial vehicles (UAVs) have become very popular in the past two decades, as developments in consumer rotorcrafts has led to lower prices for more and more advanced aircrafts. The rotorcrafts have become the most popular Vertical Take-Off and Landing (VTOL) vehicles and different from the classic helicopters, these vehicles have constant pitch blades and is controlled varying only the angular speed of each rotor. Due to its structure, these vehicles are practical prototypes for learning about aerodynamic phenomena and control of aerial vehicles. The popularity of rotorcrafts has grown so much today as it is the most used in the research field of aerial vehicles.

In applications which the UAV must be hold at stationary flight, the VTOL vehicles are the more convenient options because of their hovering capability. The attitude in a VTOL is automatically stabilized via an on-board controller in most applications, while its position is controlled by an operator through a remote-control system. Many in the research community focused on the design of position controllers for autonomous flights, resulting in remarkable advances in the field of rotor aircraft. PID controllers are the most common type of controller in many fields due to their simplicity, ease of implementation and efficiency [1-3]. If the parameters of the PID controller are not determined correctly, no matter which area of the industry is used, the system to which the controller is applied cannot perform at a satisfactory level. The use of heuristic algorithms [4-6], which is one of the algorithms developed for search purposes in many problems, has started to take on a lot of tasks related to the determination of controller parameters

***Corresponding Author:** Nihat ÇABUK, nihatcabuk@aksaray.edu.tr

[7]. Although the developed algorithms show different performances according to the structures of the systems to be controlled, most of them can give sufficient results.

In the literature, there are many studies on the control of standard UAVs such as quadrotor, hexarotor and octorotor [8-11]. Due to the proposed complicated control algorithms, which are sensitive to uncertainties in the system, stabilizing aerial vehicles is a hard task. Furthermore, tuning the gain of these controllers are also being a hard task and sometimes being time consuming. It is a known fact that system performance is affected by the nature of the commanded signal and the controller gains [12]. Incorrect selection of the commanded signal can adversely affect the overall performance of the system [13-14]. In addition, improper adjustment of controller gains can result in unsatisfactory performance. Therefore, trajectory design that directly affects the commanded signal and adjustment of controller gains should be done precisely [15].

Jabeur and Seddik [16] proposed PD and a PD-NN control schemes for a quadcopter. They stated that the PD-NN controller, which is optimized by artificial neural networks, gives excellent results against trajectory tracking and strong wind disturbances. Zareb et al. [17] used genetic algorithms to adapt and optimize the value of the controller parameters to obtain the best performance and decrease the consumed energy for Quadrotor UAV. Dewangan et al. [18] reported a solution for a path planning problem of multiple UAVs based on Grey Wolf Optimizer (GWO) algorithm. According to their results, they stated that the GWO algorithm outperforms other deterministic and meta-heuristic algorithms in path planning for 3D multiple UAVs. Shauqee et al. [19] designed a hybrid proportional double derivative and linear quadratic regulator (PD2-LQR) controller for altitude and attitude control of a quadrotor. They exploited GWO to search for optimal values of the controller's parameter. Through their simulation, they showed that the IGWO-based PD2-LQR controller can better monitor the desired reference input with shorter settling time and rise time, lower percent overshoot and minimum steady-state error and mean square error (RMSE). It can be said that the studies encountered in the literature are on the optimization of controller parameters related to multi-rotor aircraft, almost all of which have standard configurations.

In this context, this study is focused on the obtaining optimal gains of the controllers for the position and orientation control of a dodecarotor that has a unique configuration proposed previously by the authors [20-21]. For this purpose, firstly, a cascaded PID control algorithm was employed to control the vehicle. Afterwards, the gains of the controllers were tuned by using optimization techniques. At the same time, clarify the validity of the proposed method for auto-tuning the rotorcrafts controllers' gains is another impact of the study.

2. MATHEMATICAL MODELLING OF THE DODECAROTOR

2.1. Physical specifications

The UAV has 12 rotors placed in two layers to have a lower horizontal dimension. At the same time, each rotor is placed at a different angle in order to create a lifting force from twelve different notes. Thus, it is aimed to ensure that the UAV behaves more robustly in disruptive weather conditions. The solid model of the dodecarotor is given in Fig. 1.

Figure 1. Solid model of proposed dodecarotor system.

Figure 2 shows the orientation of the body, the rotational directions of the rotors, the angles and lengths of the arms, the 3D view of the vehicle and the direction of motion. Table 1 presents the physical characteristics of the proposed drone shown in Figure 2. Here, l_1 and l_2 are the arm lengths of the rotors in the upper and lower planes, respectively. Likewise, θ_1 and θ_2 are the connection angles of the upper and lower plane arm to the body, and their values are 22.5 and 45 degrees, respectively.

Table 1. Dodecarotor Physical Specifications

Parameter	Value
l1 [mm] (min-max)	660-810
l2 [mm]	450
Propeller diameter [inch] (min-max)	12-18
θ_1 [deg]	22.5
θ_2 [deg]	45
mass [kg] (min-max)	12-30
Number of rotors	4-12

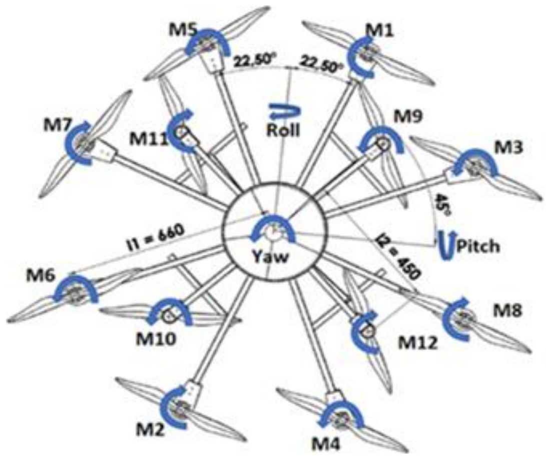

Figure 2. Physical features of proposed dodecarotor system.

2.2. Dynamic model

In order to design a controller for a system, first of all, the equation of motion is needed. The equation of motion describes the system's responses to different inputs. In our case, system inputs are the sum of rotor speeds that cause a force to control height and torques to control orientation, respectively. In order to describe this relationship, the equations of motion representing the 3D motion of the system are derived based on the Euler-Newton formulation.
A linear relationship between the body forces and the vector Ω forming the angular velocities of the motors can be obtained with a constant matrix C as in (1–3). Depending on the configuration of the vehicle, the C matrix can be calculated as in (3). The desired reaction torques and the thrust force of the rotors are represented by the vector $U_d = [T\ \tau_x\ \tau_y\ \tau_z]^T$.

$$\Omega = [\Omega_1^2 \quad \Omega_2^2 \quad \Omega_3^2 \quad \Omega_4^2 \quad \Omega_5^2 \quad \Omega_6^2 \quad \Omega_7^2 \quad \Omega_8^2 \quad \Omega_9^2 \quad \Omega_{10}^2 \quad \Omega_{11}^2 \quad \Omega_{12}^2]^T \tag{1}$$

$$C = \begin{bmatrix} k_f & k_f & k_f & k_f & k_f & k_f & k_f & k_f & k_f & k_f & k_f & k_f \\ \Lambda & -\Lambda & \Delta & \Lambda & -\Lambda & -\Delta & -\Delta & \Delta & \Gamma & -\Gamma & -\Gamma & \Gamma \\ \Delta & -\Delta & \Lambda & -\Delta & \Delta & -\Lambda & \Lambda & -\Lambda & \Gamma & -\Gamma & \Gamma & -\Gamma \\ k_m & k_m & -k_m & -k_m & -k_m & -k_m & k_m & k_m & -k_m & -k_m & k_m & k_m \end{bmatrix} \tag{2}$$

$$U_d = C * \Omega \tag{3}$$

In terms of readability of the C matrix, Λ, Δ and Γ are defined as in (4)

$$\Lambda = k_f * l_1 * \sin\theta_1 \quad \Delta = k_f * l_1 * \cos\theta_1 \quad \Gamma = k_f * l_2 * \sin\theta_2 \tag{4}$$

The proposed UAV is driven by a net force consisting of three components: thrust generated by the rotors, gravitational forces and external disturbance forces. The drag force caused by the drone body has not been taken into account since it is very low compared to these forces. The net force acting on the system is given in F_b (5). The translational acceleration caused by F_b is as in (6).

$$F_b = T - ({}^B R_G * mg + F_d) \tag{5}$$

$$\dot{V}_b = \frac{F_b}{m} - (\omega_b \text{ x } V_b) \tag{6}$$

where V_b and $\omega_b = [p\ q\ r]^T$ are translational and angular velocity vectors defined in the body frame, respectively. These velocities can be estimated with Inertial Measurement Unit (IMU) feedback.

Different magnitudes of thrust in the rotors cause roll and pitch moments in the system. There are also gyroscopic moments that occur in the direction perpendicular to the rotational motion of each rotor due to the change in the orientation of the rotor's rotation. In (7), the total net moment M_b acting on the system is given. Since the magnitudes of the gyroscopic moments due to the angular acceleration of the rotors is very low compared to body torques, they can be neglected. The angular acceleration caused by M_b is as in (9).

$$M_b = \tau_{gyr} + \tau_{x,y,z} \tag{7}$$

$$M_b = \begin{bmatrix} \sum_{i=1}^{n_r} -(-1)^i * (I_{zz} * p * \Omega_i) \\ \sum_{i=1}^{n_r} (-1)^i * (I_{zz} * q * \Omega_i) \\ \sum_{i=1}^{n_r} -(-1)^i * (I_{zz} * \dot{\Omega}_i) \end{bmatrix} + \begin{bmatrix} \tau_x \\ \tau_y \\ \tau_z \end{bmatrix} \tag{8}$$

$$I\dot{\omega}_b = (M_b - (\omega_b \text{ x } (I\omega_b)) \tag{9}$$

The Euler velocities $\dot{\varphi}$ and the angular velocity vector ω_b are correlated by a kinematic connection: $\omega_b = \xi_\varphi \dot{\varphi}$, where ξ_φ expresses a matrix that is relating the Euler velocities with the body angular rates. Subsequently, first derivative of this equation yields $\dot{\omega}_b = \xi_\varphi \ddot{\varphi} + \dot{\xi}_\varphi {\xi_\varphi}^{-1} \omega_b$. This fact and (9) yields (10).

$$M(\varphi)\ddot{\varphi} = -C(\varphi, \dot{\varphi})\dot{\varphi} + M_b \tag{10}$$

where $M(\varphi)$ and $C(\varphi, \dot{\varphi})$ denotes the full inertia matrix and the Coriolis matrix, respectively. In theory, due to the fact that the motion of a VTOL vehicle during hover is drastically separated in each axis, the Coriolis matrix becomes very small and therefore negligible. According to the assumptions made, the simplified non-linear equation of motion of the proposed dodecarotor is obtained as follows.

$$\begin{aligned} m\ddot{x} &= -(u + w_x)sin\theta \\ m\ddot{y} &= (u + w_y)cos\theta sin\phi \\ m\ddot{z} &= (u + w_z)cos\theta cos\phi - mg \\ I_x\ddot{\theta} &= \tau_x + w_\theta \\ I_y\ddot{\phi} &= \tau_y + w_\phi \\ I_z\ddot{\psi} &= \tau_z + w_\psi \end{aligned} \tag{11}$$

where x, y and z are the positions of the tool in Cartesian coornidates. u defines the total thrust. τ_z, τ_y and τ_x are yaw, pitch, roll moments, respectively. Likewise, θ, ϕ and ψ are roll, pitch and yaw angles, respectively. I_j and g are the inertia matrix and gravitational acceleration, respectively. Finally, w_k indicates unknown disturbances on the corresponding axis.

3. PROBLEM FORMULATION

3.1. Controller design

The PID proportional-integral-derivative controller control loop method is a widely used feedback controller method in industrial control systems. A PID controller continuously calculates the error value, which is the difference between the desired system state and the actual system state. Depending on the requirement of the system to be controlled, one, two or three of these three control units (P, I, D) are used. First of all, the mathematical model of the system to be controlled is obtained. A controller structure is constructed for each variable to be controlled.

The simplified form of the VTOL dynamic model obtained in (11) is given in (12).

$$\ddot{\varphi} = u_\varphi + w_\varphi \tag{12}$$

where $\ddot{\varphi}$ states the second derivative of the Euler angles and u defines the control inputs. Here, w states external disturbances. The desired controller inputs specified in (13) is sufficient to balance the second order system given in (12), for the most part, if the disturbances are neglected.

$$u_{\varphi} = -k_p e(t) - k_d \frac{de(t)}{dt} \quad (13)$$

Where, $e(t)$ is the error between desired value and the actual states. Likewise, k_p is the proportional gain and k_d is the derivative gain. In order that the change rate of the error does not trigger the derivative kick phenomenon due to the sudden change in the desired state, the change of the state is used here, not the error.

The angular rates $\dot{\varphi}$ are estimating from the IMU feedback, as mentioned before. Following this idea, the control algorithm used in this study can be deduced from (13) as given in (14). Since the stability analysis of the closed-loop system (14) is obvious, a separate analysis was not carried out in this study.

$$u(t) = k_p e(t) - k_d \dot{\varphi} \quad (14)$$

3.2. Optimization problem statement

In (14) the proportional and the derivative gains need to be tuned. In the literature, there exists several methods that use the phase domain and the time domain characteristics to adjust PID gains. In this study, an optimization procedure is adopted to adjust the controller gains in the time domain. For this purpose, an objective function is defined as in (15), which is based on the time domain characteristics.

$$\Phi_{PD} = \min \sum (a_1 (t_s - t_i)^2 + a_2 M_o^2) \quad (15)$$

Table 2. GWO and PSO Parameters

Parameter	Number of search agents	Max. iterations	Lower bound	Upper bound
Value	30	100	0	100

where the constants denoted by a_i define the weight of the relevant parameter. t_s and t_i are the settling time and the desired settling time. M_o is defined as the Maximum Overshoot. By defined objective function in (15), without an overshoot a fast-settling time is aimed.

3.3. Methodology to solve optimization problem

Grey Wolf Optimizer (GWO) that is a new meta-heuristic search algorithm is implemented to solve the optimization problem [18, 22-23] that defined in (15). GWO algorithm mimics the leadership hierarchy and hunting mechanism of grey wolves in nature. The algorithm was first developed by Mirjalili et. al. in 2014 [24]. In addition, Particle Swarm Optimizer, which is the most popular Swarm Intelligence techniques, is also implemented to benchmark the obtained results from GWO. A more detailed description about GWO and PSO can be found in [7, 23-24].

The system and the proposed controller were developed using Matlab and Simulink, which has the powerful tools for simulations. The integrated structure of Matlab and Simulink environments enables online data exchange during the optimization process between phases. To obtain the time domain response characteristics required to evaluate the objective function described in (15), the closed loop system is simulated in the Simulink environment using possible solutions determined by the proposed algorithms running in the Matlab environment. To obtain system response a step reference input is used in the simulation study. Finally, weights a_1 and a_2 in the defined objective function in (15) are set to 10 and 0.5, and the simulation time is limited to 10 s.

The optimized PD controller parameters shown in Table 3 are applied to the system to evaluate the proposed method. These simulations are performed in two cases; first for a ramp input response and then for a predefined trajectory.

In order for the system to be fully simulated in the Simulink environment, the mathematical model of the system must be created correctly. The physical properties of the components of the vehicle, such as the mass of the vehicle and the inertial values, which are the parameters in this model, should be determined close to the truth. The Simulink model of all dodecarotor UAV created according to these determined parameters is given in figure 4.

4. SIMULATION RESULTS AND CASE STUDIES

Optimization process is performed 100 times separately for both algorithms using parameters defined in Table 2. Each optimization process is continued up to 30 iterations or until a solution reaching the $\Phi_{PD} \leq 0.001$ condition. Comparison of the proposed algorithms in terms of converges performances is given in Figure 3. As seen in the figure, GWO offers better convergence performance although both algorithms run with the exact same parameter. The optimized PD controller parameters shown in Table 3 are applied to the system to evaluate the proposed method. These simulations are performed in two cases; first for a ramp input response and then for a predefined trajectory.

Table 3. PD Controller Gains

States		Roll		Pitch		Altitude	
		k_p	k_d	k_p	k_d	k_p	k_d
Gains	GWO	16.89	46.04	17.43	24.69	2.04	47.64
	PSO	5.18	6.90	8.72	22.14	3.38	98.92

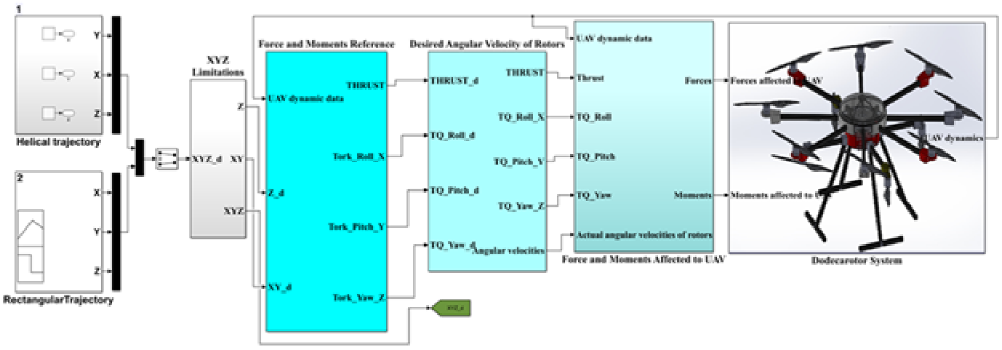

Figure 4. Simulink model of dodecarotor system

4.1. Ramp reference tracking

Ramp reference inputs are applied to the positions of the system at different simulation time. The tracking performance in all axes are given in the Figure 5. As seen in the figure, the aim of the study that is tuning the gains for a fast-settling time without overshoot is satisfied.

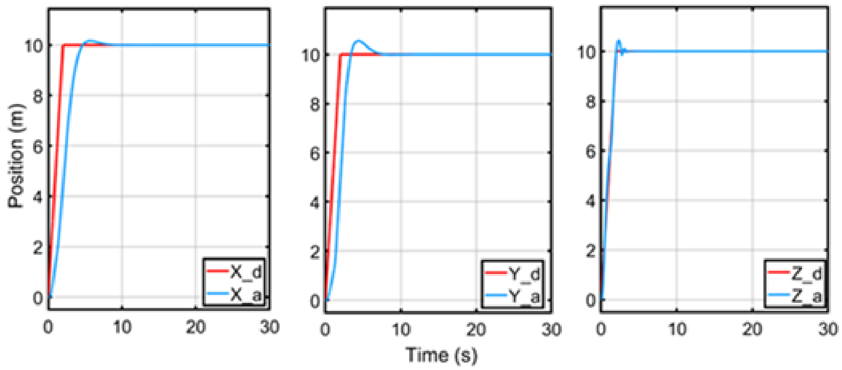

Figure 5. Reference tracking performance for all axes (left – X-axis, middle – Y-axis and right– Z-axis.)

By these results, it can be concluded that GWO provides successful and fast results in optimizing the gains of a PD controller that is designed for the Dodecarotor.

4.2. Trajectory tracking

In this section, the output responses of the case studies with pre-defined trajectories to test the Dodecarotor system using optimized PD controllers are presented. The trajectories studied in this section were carefully chosen to reflect the difficulties the control system may encounter in executing the required tracking.

The first performed case is a rectangular trajectory. Figure 6 demonstrates the tracking performance of the Dodecarotor system for the rectangular trajectory. As can be seen in the Figure 6, Dodecarotor followed the trajectory successfully with a tolerable error in the corners. Since the trajectory changes its direction suddenly at certain times in the corners, the errors in the corners can be considered tolerable.

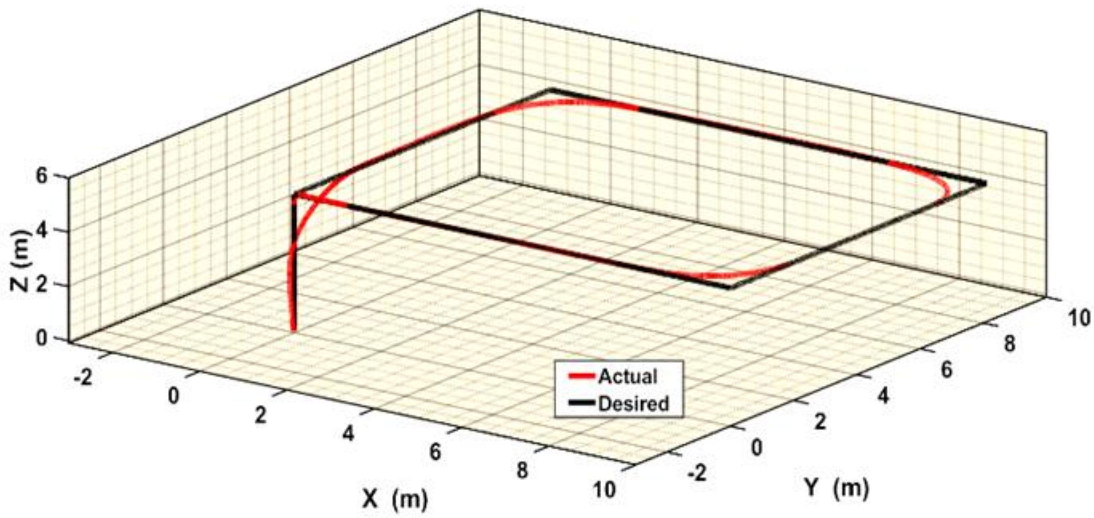

Figure 6. Rectangular trajectory tracking performance of the Dodecarotor system (Black line – Desired path, Red line – Actual path.).

The second performed case is a helical-shaped trajectory. Figure 7 demonstrates the tracking of the Dodecarotor system for the rectangular trajectory. As can be seen in the Figure 7, Dodecarotor followed the trajectory successfully.

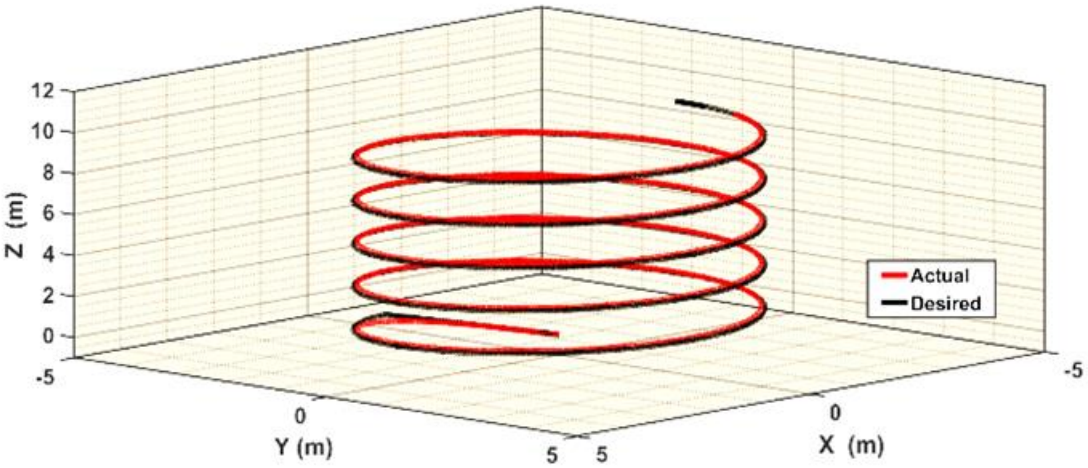

Figure 7. Helical trajectory tracking performance of the Dodecarotor system (Black line – Desired path, Red line – Actual path.).

The RMS values of the position errors in the three axes that occur in both rectangular and helical trajectories tracking are given in table 4. The results are shown in the table, taking into account the different mass values of the vehicle in the simulations performed with the controller gains obtained with both optimizers.

Table 4. RMSE values of reference trajectories

Parameters		Rectangular trajectory			Helical trajectory		
Optimizer	**Mass [kg]**	**X**	**Y**	**Z**	**X**	**Y**	**Z**
GWO	12	1.4720	1.1910	0.1567	0.9290	0.9970	0.0303
	18	1.4720	1.1910	0.1591	0.9290	0.9970	0.0310
	24	1.4720	1.1910	0.1619	0.9292	0.9970	0.0317
	30	1.4730	1.1910	0.1651	0.9292	0.9971	0.0325
PSO	12	1.4740	1.1940	0.2612	0.9311	0.9973	0.0519
	18	1.4960	1.1940	0.2705	0.9311	0.9976	0.0544
	24	1.4770	1.1950	0.2813	0.9320	0.9977	0.0574
	30	1.4775	1.1950	0.2930	0.9325	0.9978	0.0607

From the results, it can be concluded that the validity of the approach implemented to tune the gains of the PD control that is applied to a Dodecarotor system is valid.

5. CONCLUSION

In this study, a fully mathematical model of a Dodecarotor with a unique configuration is adopted to design and tune a PD controller for stabilization and trajectory tracking for this complex, unstable and highly non-linear system. GWO, which is a widely used optimization algorithm in many systems in recent years, has been applied to adjust the controller gains. Compared to other commonly used optimizer, PSO. Simulations were performed for both optimizers. The simulations were made for two different trajectories and 4 different situations, and the RMS values of the position errors obtained from the simulations were used for this comparison. With the optimized controller parameters, the trajectory tracking performances of the UAV at 12 kg mass (no payload), 18 kg mass, 24 kg mass and 30 kg mass (full payload) in both rectangular and helical trajectory were evaluated. The results of the evaluations are presented both graphically and numerically. The obtained results can be briefly expressed as follows.

- The performance in helical trajectory tracking was better in the test performed with the controller gains obtained with both optimizers.
- The trajectory tracking performance decreased slightly as the vehicle's mass increased in all the controller gain values obtained with both optimizers.
- GWO provides a better convergence performance than PSO in both different mass and trajectory cases.
- When the numerical results given in Table 4 are examined, it is seen that using the parameters obtained with GWO, there is a decrease of 40-46% in axis position errors compared to PSO in UAVs with four different masses.

Finally, with the performed simulation results, the designed and optimized controller has been proven to balance the Dodecarotor system and to perform the required tracking.

Declaration of Ethical Standards

Not applicable.

Credit Authorship Contribution Statement

Şahin Yıldırım: Conceptualization, Resources, Writing - Review & Editing.
Nihat Çabuk: Conceptualization, Methodology, Investigation, Writing- Original draft preparation.
Veli Bakırcıoğlu: Conceptualization, Methodology, Investigation, Writing- Original draft preparation.

Declaration of Competing Interest

The authors declare that they have no known competing financial interests or personal relationships that could have appeared to influence the work reported in this paper.

Funding / Acknowledgements

This study was supported by Erciyes University Scientific Research Projects Unit within the scope of FBA-2017-7393 project.

Data Availability

The dataset generated during the current study are available from the corresponding author on reasonable request.

REFERENCES

[1] D. Kotarski, Z. Benic, and M. Krznar, "Control Design for Unmanned Aerial Vehicles with Four Rotors," *Interdiscip. Descr. Complex Syst.*, vol. 14, no. 2, pp. 236–245, 2016.

[2] N. Hadi and A. Ramz, "Tuning of PID Controllers for Quadcopter System using Hybrid Memory based Gravitational Search Algorithm – Particle Swarm Optimization," *Int. J. Comput. Appl.*, vol. 172, no. 4, pp. 9–18, 2017.

[3] M. Akhil, M. Krishna Anand, A. Sreekumar, and P. Hithesan, "Simulation of the mathematical model of a quad rotor control system using Matlab Simulink," *Appl. Mech. Mater.*, vol. 110–116, no. October 2011, pp. 2577–2584, 2012.

[4] M. Ayyıldız and K. Çetinkaya, "Comparison of four different heuristic optimization algorithms for the inverse kinematics solution of a real 4-DOF serial robot manipulator," *Neural Comput. Appl.*, vol. 27, no. 4, pp. 825–836, 2016.

[5] M. B. Çetinkaya, H. Duran, and T. Hanne, "Performance Comparison of Most Recently Proposed Evolutionary, Swarm Intelligence, and Physics-Based Metaheuristic Algorithms for

Retinal Vessel Segmentation," *Math. Probl. Eng.*, vol. 2022, 2022.
[6] M. Mahi, O. K. Baykan, and H. Kodaz, "A new approach based on particle swarm optimization algorithm for solving data allocation problem," *Appl. Soft Comput. J.*, vol. 62, pp. 571–578, 2018.
[7] M. A. Sen and M. Kalyoncu, "Grey wolf optimizer based tuning of a hybrid LQR-PID controller for foot trajectory control of a quadruped robot," *Gazi Univ. J. Sci.*, vol. 32, no. 2, pp. 674–684, 2019.
[8] M. Moussid, A. Sayouti, and H. Medromi, "Dynamic Modeling and Control of a HexaRotor using Linear and Nonlinear Methods," *Int. J. Appl. Inf. Syst.*, vol. 9, no. 5, pp. 9–17, 2015.
[9] S. Li, Y. Wang, J. Tan, and Y. Zheng, "Adaptive RBFNNs/integral sliding mode control for a quadrotor aircraft," *Neurocomputing*, vol. 216, pp. 126–134, 2016.
[10] Y.-R. Tang, X. Xiao, and Y. Li, "Nonlinear dynamic modeling and hybrid control design with dynamic compensator for a small-scale UAV quadrotor," *Measurement*, vol. 109, pp. 51–64, Oct. 2017.
[11] Ş. Yıldırım, N. Çabuk, and V. Bakırcıoğlu, "Comparison of Flight Performances of Unmanned Air Vehicle with Six Rotors and Eight Rotors Under Different Disturbance Effects," *Konya J. Eng. Sci.*, vol. 8, no. 3, pp. 552–562, 2020.
[12] R. Miranda-Colorado, L. T. Aguilar, and J. E. Herrero-Brito, "Reduction of power consumption on quadrotor vehicles via trajectory design and a controller-gains tuning stage," *Aerosp. Sci. Technol.*, vol. 78, pp. 280–296, 2018.
[13] W. Dong, G. Y. Gu, X. Zhu, and H. Ding, "A high-performance flight control approach for quadrotors using a modified active disturbance rejection technique," *Rob. Auton. Syst.*, vol. 83, pp. 177–187, 2016.
[14] R. Miranda-Colorado and L. T. Aguilar, "Robust PID control of quadrotors with power reduction analysis," *ISA Trans.*, vol. 98, no. xxxx, pp. 47–62, 2020.
[15] H. Yao, R. Qin, and X. Chen, "Unmanned aerial vehicle for remote sensing applications - A review," *Remote Sens.*, vol. 11, no. 12, pp. 1–22, 2019.
[16] C. Ben Jabeur and H. Seddik, "Neural networks on-line optimized PID controller with wind gust rejection for a quad-rotor," *Int. Rev. Appl. Sci. Eng.*, 2021.
[17] M. Zareb, W. Nouibat, Y. Bestaoui, R. Ayad, and Y. Bouzid, "Evolutionary Autopilot Design Approach for UAV Quadrotor by Using GA," *Iran. J. Sci. Technol. - Trans. Electr. Eng.*, vol. 44, no. 1, pp. 347–375, 2020.
[18] R. K. Dewangan, A. Shukla, and W. W. Godfrey, "Three dimensional path planning using Grey wolf optimizer for UAVs," *Appl. Intell.*, vol. 49, no. 6, pp. 2201–2217, 2019.
[19] M. N. Shauqee, P. Rajendran, and N. M. Suhadis, "Proportional Double Derivative Linear Quadratic Regulator Controller Using Improvised Grey Wolf Optimization Technique to Control Quadcopter," *Appl. Sci.*, vol. 11, no. 6, p. 2699, Mar. 2021.
[20] Ş. Yıldırım, N. Çabuk, and V. Bakırcıoğlu, "Design and trajectory control of universal drone system," *Measurement*, vol. 147, p. 106834, Dec. 2019.
[21] V. Bakırcıoğlu, N. Çabuk, and Ş. Yıldırım, "Experimental comparison of the effect of the number of redundant rotors on the fault tolerance performance for the proposed multilayer UAV," *Rob. Auton. Syst.*, vol. 149, p. 103977, Mar. 2022.
[22] M. N. Shauqee, P. Rajendran, and N. M. Suhadis, "An effective proportional-double derivative-linear quadratic regulator controller for quadcopter attitude and altitude control," *Automatika*, vol. 62, no. 3–4, pp. 415–433, 2021.
[23] M. Karakoyun, A. Ozkis, and H. Kodaz, "A new algorithm based on gray wolf optimizer and shuffled frog leaping algorithm to solve the multi-objective optimization problems," *Appl. Soft Comput. J.*, vol. 96, p. 106560, 2020.
[24] S. Mirjalili, S. M. Mirjalili, and A. Lewis, "Grey Wolf Optimizer," *Adv. Eng. Softw.*, vol. 69, pp. 46–61, Mar. 2014.